Journal of Alloys and Compounds 806 (2019) 1047–1051

Contents lists available at ScienceDirect

Journal of Alloys and Compounds

journal homepage: http://www.elsevier.com/locate/jalcom

Conventional and inverse barocaloric effects in ferroelectric NH_4HSO_4

Mikhail V. Gorev [a, b], Ekaterina A. Mikhaleva [a, b], Igor N. Flerov [a, b, *], Evgeniy V. Bogdanov [a, c]

[a] Kirensky Institute of Physics, Federal Research Center KSC SB RAS, Krasnoyarsk, Russia
[b] Institute of Engineering Physics and Radioelectronics, Siberian Federal University, Krasnoyarsk, Russia
[c] Institute of Engineering Systems and Energy, Krasnoyarsk State Agrarian University, 660049, Krasnoyarsk, Russia

ARTICLE INFO

Article history:
Received 17 April 2019
Received in revised form
22 July 2019
Accepted 22 July 2019
Available online 29 July 2019

Keywords:
Polymorphic phase transformation
Phase diagram
Order–disorder phenomena
Entropy
Barocaloric effect
PACS: 62.50.-p
65.40.-b
81.30.-t

ABSTRACT

In this study, the conventional and inverse barocaloric effects (BCE) in ferroelectric NH_4HSO_4 are reported. Maximum extensive and intensive BCE near order–disorder phase transition can be achieved at low pressure $p \leq 0.1$ GPa. Large thermal expansion of the crystal lattice plays a very important role in the developing conventional BCE and conversation between BCE of different sign in the narrow temperature range.

1. Introduction

In recent years, much attention is paid to caloric effects (CE) in solids, particularly in ferroics, associated with the reversible change in the temperature, ΔT_{AD}, or entropy, ΔS_{CE}, under variation of the external field in adiabatic and isothermal conditions, respectively [1–4]. One of the main reasons for this interest is related to the possibility to use the materials showing large CE's as solid state refrigerants in alternative cooling cycles [5–8]. Among the CEs of different physical nature, the barocaloric effect (BCE) is distinguished by a serious advantage associated with its universality. Indeed, both extensive ΔS_{BCE} and intensive ΔT_{AD} barocaloric parameters strongly depend on the volume thermal expansion $(\partial V/\partial T)_p$ which very often shows large change near the temperature of any phase transitions: ferroelectric, ferroelastic, ferromagnetic

$$\Delta S_{BCE} = -\int_0^p \left(\frac{\partial V}{\partial T}\right)_p dp, \quad \Delta T_{AD} = -\frac{T}{C_p}\Delta S_{BCE}, \tag{1}$$

where C_p is the heat capacity.

The most intensively, BCE was studied in materials undergoing ferroelastic [9,10] and ferromagnetic [11–14] phase transitions. As to the ferroelectrics, their barocaloric efficiency was investigated only sporadically [11,15–17]. It is known that the values and behavior of the BCE depend on the behavior and change in the entropy ΔS of the phase transition as well as on the sensitivity of the phase transition temperature to hydrostatic pressure [9,10]. Thus, ferroics undergoing order–disorder transformations accompanied by large change in the volume and as result in baric coefficient, $dT_0/dp = \delta V/\delta S$, are the most promising barocaloric materials. Important requirements for caloric materials are also their low cost and ecological tolerance.

It has recently been shown that ferrielectric $(NH_4)_2SO_4$ meets all of the above requirements [15]. Due to significant values of $\Delta S = 17$ J/mol·K $\approx R \ln 8$ and $dT_0/dp = -45$ K/GPa, rather large extensive and intensive BCE were observed in the region of the phase transition $Pnam - Pna2_1$ under low pressure. In accordance

* Corresponding author. Kirensky Institute of Physics, Federal Research Center KSC SB RAS, Krasnoyarsk, Russia.
E-mail addresses: gorev@iph.krasn.ru (M.V. Gorev), katerina@iph.krasn.ru (E.A. Mikhaleva), flerov@iph.krasn.ru (I.N. Flerov), evbogdanov@iph.krasn.ru (E.V. Bogdanov).

https://doi.org/10.1016/j.jallcom.2019.07.273
0925-8388/

with Eq. (1), the negative baric coefficient associated with the negative value $(\partial V/\partial T)_p$ is the reason of the inverse BCE_{inv} in $(NH_4)_2SO_4$ accompanied by increase/decrease in entropy/temperature under pressure increase. It was also found that large coefficient of the volume thermal expansion of the crystal lattice, β_{LAT}, can play an important role in formation of real BCE in material. Indeed, in the case of ammonium sulphate, large positive value $\beta_{LAT} = 1.4 \times 10^{-4}$ K^{-1} leads to decrease in the inverse BCE_{inv} under pressure due to the appearance of the conventional contribution BCE ($\Delta S_{BCE} < 0, \Delta T_{AD} > 0$) [15]. The conversion from BCE_{inv} to BCE_{conv} was observed in a narrow temperature range. When pressure increases, the ratio between these values changes and at $p = 0.25$ GPa is about $BCE_{conv}/BCE_{inv} = 0.15$. Thus, to get correct information on BCE in materials with large thermal expansion coefficient, it is necessary to take into account the effect of pressure on the lattice entropy. It is obvious that the magnitude of baric coefficient strongly effects on the maximum value of the intensive BCE [18]. In this respect, it is interesting to analyze both BCE in material with anomalously large negative or positive dT/dp. From this point of view, another ferroelectric crystal, ammonium hydrogen sulphate, is very good example.

Indeed, NH_4HSO_4 undergoes two successive phase transitions $P2_1/c \leftrightarrow Pc \leftrightarrow P1$, of the strong second and first order at $T_1 = 271$ K and $T_2 = 159$ K, respectively. One more difference is that anomaly of volumetric thermal expansion coefficient is positive at T_1 and negative at T_2 [19] which leads to BCE_{conv} and BCE_{inv}. Thus, the contribution from the thermal expansion of the crystal lattice to both BCE will be also different. Despite the large difference in the entropy of the phase transitions (ΔS_1=1.2 J/mol•K, $\Delta S_2 = 7.6$ J/mol•K), one can suppose that BCE_{conv} at T_1 could be strongly increased due to rather large value of $\beta_{LAT} = 2\times10^{-4}$ K^{-1} far from the phase transition points. In addition, like $(NH_4)_2SO_4$, ammonium hydrogen sulphate is also easy to prepare, cheap and environmentally friendly.

In the present paper, we performed an analysis of extensive and intensive barocaloric efficiency of NH_4HSO_4 near both phase transformations based on methods developed by us earlier [18]. For this aim, the dependencies of $\Delta T_{AD}(T,p)$ and $\Delta S_{BCE}(T,p)$ were determined using data on total and anomalous heat capacity [19], the $T-p$ phase diagram and the dependencies of entropy of the phase transitions on temperature and pressure.

2. Experimental details

Powder samples of ammonium hydrogen sulphate were obtained by slow evaporation at 45°C from an aqueous solution containing equimolar quantities of high purity raw materials $(NH_4)_2SO_4$ and H_2SO_4.

The quality of samples used for the experiments was checked at room temperature using XRD, which revealed a monoclinic symmetry consistent with the space group $P2_1/c$ ($Z = 8$) suggested in Refs. [20,21]. No additional phases were observed in the samples. Fig. 1 shows the results of Rietveld refinement (R_{wp}=6.04, $R_p = 4.23$, $\chi^2 = 2.06$). The unit cell parameters $a = 24.770(6)$Å, $b = 4.611(1)$Å, $c = 14.871(4)$Å, $\beta = 89.70(1)$ grad are consistent with the values determined in Ref. [21].

Quasi-ceramic samples of NH_4HSO_4 in the form of disks, approximately 1.0 mm thick and approximately 6 mm in diameter, were used for investigations. Because of the presence of ammonium ion in crystal, the heat treatments of ceramics were not performed. For dielectric measurements, electrodes on pellets were formed by conducting glue covered the opposite sides of the sample.

The effect of hydrostatic pressure on temperature and entropy of the phase transitions was studied using a piston-cylinder type vessel associated with a pressure multiplier. Pressure of up to 0.25 GPa was generated using a mixture of silicon oil and pentane exhibiting optimal electrical and heat conductivity, solidification point and viscosity as the pressure-transmitting medium. Pressure and temperature were measured using a manganin resistive sensor and a copper-constantan thermocouple, with accuracies of about ± 10^{-3} GPa and ±0.3 K respectively.

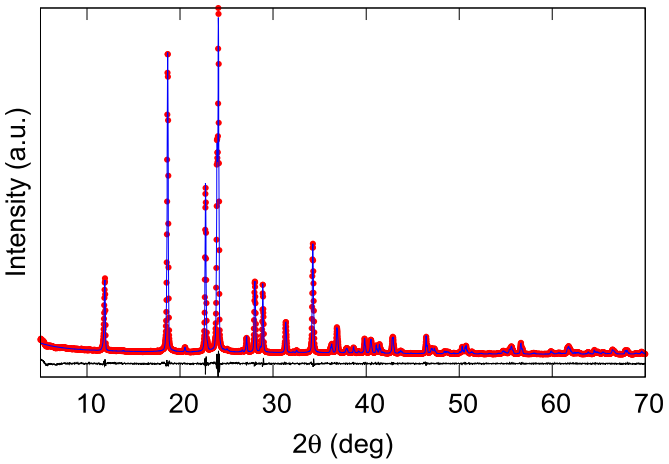

Fig. 1. Difference Rietveld plot for NH_4HSO_4 at room temperature.

The dependencies $T_1(p)$ and $T_2(p)$ were revealed, firstly, in experiments with differential thermal analysis (DTA) and, secondly, by measurements of the permittivity ε. In the former case, to detect anomalies of DTA-signal associated with the heat capacity anomalies, high-sensitive differential copper–germanium thermocouple was used. In the latter case, experiments were performed using an E7-20 immittance meter. To ensure the reliability of the results, the measurements were performed for both increasing and decreasing pressure cycles.

3. Results and discussion

At ambient pressure, the anomalies of DTA signal and ε were detected at about $T_1 = 271.5\pm1.0$ K and $T_2 = 160\pm2$ K (Fig. 2 (a) and (b)), which agree well with values observed during measurements of the heat capacity [19]. Fig. 2(c) shows that an increase in pressure leads to linear increase and decrease in T_1 and T_2, respectively: $dT_1/dp = +90\pm15$ K/GPa and $dT_2/dp = -123\pm15$ K/GPa which are significantly higher than that for ammonium sulphate [15].

Due to the limited sensitivity of the DTA method, the area under the DTA peak at T_2 represents a change in the enthalpy δH_2 (entropy $\delta S_2 = \delta H_2/T_2$) jump at the first order phase transition $Pc \leftrightarrow P1$ in NH_4HSO_4. An increase in pressure is accompanied by a linear decrease in the value of δS_2 which reaches zero at $p \approx 0.17$ GPa (Fig. 2(d)) that can be considered as corresponding to the pressure of the tricritical point. On the other hand, it is unlikely that such a low pressure may affect the degree of disordering of structural elements in phases $P2_1/c$ and Pc, and as a result the total entropy change at the $Pc \leftrightarrow P1$ transformation, $\Delta S_2(p) = \delta S_2(p) + \Delta S_2^*(T,p)$, remains constant. Here $\Delta S_2^*(T,p)$ is the temperature- and pressure-dependent contribution.

The analysis of extensive and intensive BCE in NH_4HSO_4 was performed in three steps.

At the first stage, the possible influence of pressure on the entropy of the crystal lattice ΔS_{LAT} was not taken into account. Fig. 3 demonstrates the temperature behavior of the lattice $S_{LAT}(T) - S_{LAT}(100\,\mathrm{K}) = \int_{100}^{T}(C_{LAT}/T)dT$ and total $S = \int_{100}^{T}(C_p/T)dT$ entropies in the vicinities of T_1 and T_2. Temperature dependencies $S(T)$ under

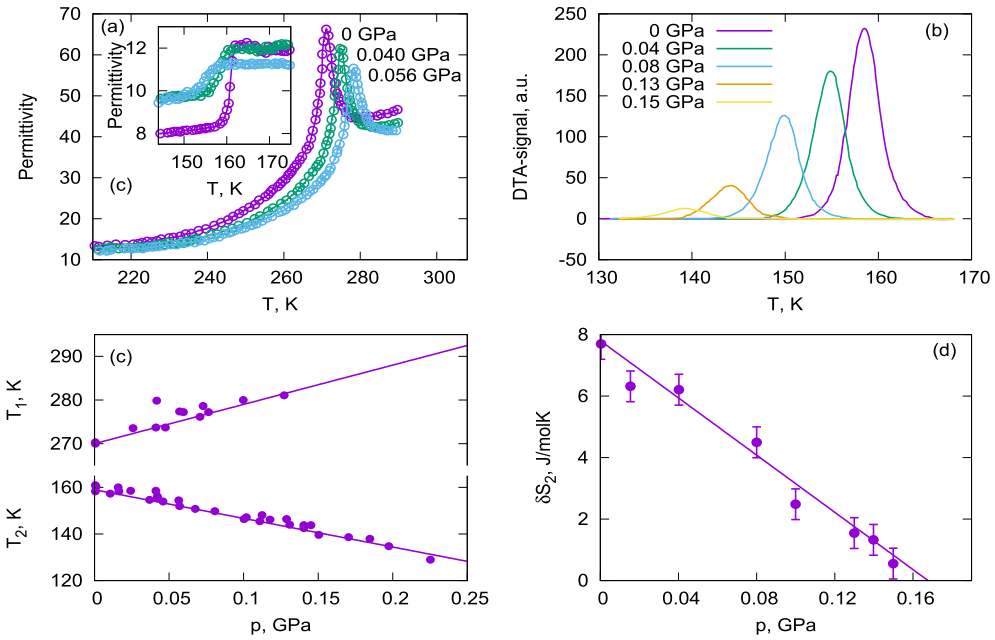

Fig. 2. (a) Temperature dependencies of permittivity for NH_4HSO_4 around T_1 and T_2 and (b) anomalous component of the DTA signal near T_2 at different hydrostatic pressure. (c) Temperature – pressure phase diagram combining the results on the DTA signal and permittivity study. (d) Entropy jump δS_2 for the first–order transition in NH_4HSO_4 at different hydrostatic pressure.

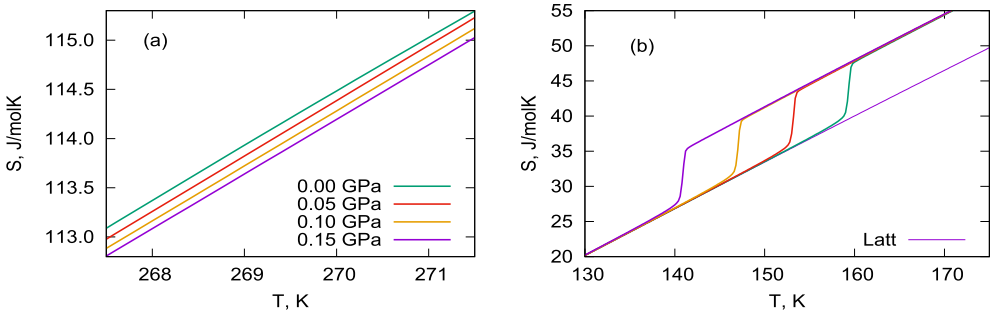

Fig. 3. Temperature dependencies of total entropy of NH_4HSO_4 at different hydrostatic pressure near (a) T_1 and (b) T_2.

pressure were determined by summation of the lattice entropy S_{LAT} and the anomalous contributions ΔS_1 and ΔS_2 shifted along the temperature scale in accordance with the sign of baric coefficients dT_1/dp and dT_2/dp. The values and behavior of extensive BCE, ΔS_{BCE}, at different pressure were determined from temperature dependencies of the total entropy as a difference $\Delta S_{BCE} = S(T,p) - S(T,p=0)$ at constant temperature (Fig. 4(a)). The temperature dependencies of the intensive BCE were revealed analyzing plots of $S(T,p) = S_{LAT}(T,p=0) + \Delta S(T,p)$ at constant entropy $S(T,p) = S(T+\Delta T_{AD}, p=0)$ (Fig. 4(b)). Large difference in BCE at T_1 and T_2 at the same pressure is the result of the different values of ΔS_1 and ΔS_2.

It is known [22] that if we neglect the contribution of the thermal expansion of the crystal lattice, the maximum values of both BCE are limited by the value of the entropy of the phase transition: $(\Delta S_{BCE}^{max})_{T1} = \Delta S_1 = -10$ J/kg·K, $(\Delta T_{AD}^{max})_{T1} = 2$ K; $(\Delta S_{BCE}^{max})_{T2} = \Delta S_2 = 68$ J/kg·K, $(\Delta T_{AD}^{max})_{T2} = 12$ K. However, undoubtedly important is the ability to realize in the material maximum values of both BCE at low pressure.

Estimates made using the following relation $p_{min} = T\Delta S/(C_{LAT}dT/dp)$, valid for phase transitions of the first order [9], show that the value $(\Delta S_{BCE}^{max})_{T2}$ can be implemented in NH_4HSO_4 by rather insignificant pressure 0.1 GPa. In fact, the rather large value $(\Delta S_{BCE})_{T2} = 0.95(\Delta S_{BCE}^{max})_{T2}$ can be achieved even at much lower pressure, $p \approx 0.02$ GPa (Fig. 4(a)). However, intensive BCE, which also depends on the dS_{LAT}/dT derivative, is characterized by lower increase rate under pressure and reaches $(\Delta T_{AD}^{max})_{T2}$ at about 0.13 GPa (Fig. 4(b)). As to the second order phase transition, at pressure 0.1 GPa extensive and intensive effects reach only about 18% of $(\Delta S_{BCE}^{max})_{T1}$ and $(\Delta T_{AD}^{max})_{T1}$.

At the second stage, effect of the lattice entropy change under pressure on BCE in NH_4HSO_4 was studied. This contribution can be evaluated using Maxwell relation $(\partial S_{LAT}/\partial p)_T = -(\partial V/\partial T)_p$

$$\Delta S_{LAT}(T,p) = -\int_0^p (\partial V/\partial T)_p dp \approx -V_m \beta_{LAT}(T) p. \quad (2)$$

here $V_m = 6.17 \times 10^{-5}$ m^3/mol) is the molar volume.

Taken into account the data of the thermal expansion study of the related $(NH_4)_2SO_4$ [15], it was suggested that the values of β_{LAT} and V_m of NH_4HSO_4 are also weakly depend on the pressure. Lattice contribution was determined from the results of dilatometric study of NH_4HSO_4 [19].

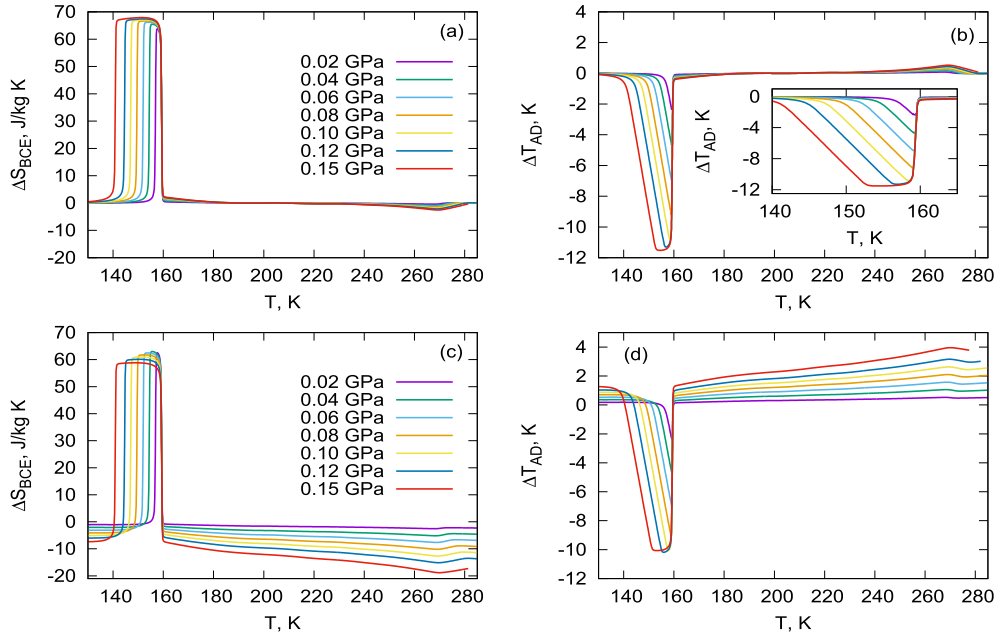

Fig. 4. (a) Barocaloric entropy and (b) adiabatic temperature changes at different hydrostatic pressure in a wide temperature range determined without taking into account the effect of thermal expansion of the crystal lattice. Effect of thermal expansion of the crystal lattice on (c) ΔS_{BCE} and (d).ΔT_{AD}

Fig. 4(c) and (d) demonstrate that due to the same sign of both derivatives, $(\partial V/\partial T)_{T1}$ and $(\partial V_{LAT}/\partial T)$, there is a strong increase in BCE_{conv}. At $p = 0.15$ GPa, the values $(\Delta S_{BCE})_{T1} = -18.8\pm1.5$ J/kg•K and $(\Delta T_{AD})_{T1} = 4.0\pm0.2$ K are about one and a half times higher than even the maximum values considered above as associated with the phase transition entropy ΔS_1. Thus, contributions of $(\Delta S^{LAT}_{BCE})_{T1}$ and $(\Delta T^{LAT}_{AD})_{T1}$ to the full BCE at T_1 are predominant.

On the other hand, at the same pressure, BCE_{inv} associated with the phase transition $Pc - P1$ ($(\partial V/\partial T)_{T2} < 0$), is reduced to the magnitudes $(\Delta S_{BCE})_{T2} = 59\pm5$ J/kg•K, $(\Delta T_{AD})_{T2} = -\ 10.0\pm\ 0.8$ K by BCE^{LAT}_{conv} arising in accordance with Eq. (2), $(\partial V_{LAT}/\partial T) > 0$: $(\Delta S^{LAT}_{BCE})_{T2} = -9.0\pm0.7$ J/kg•K, $(\Delta T^{LAT}_{AD})_{T2} = 1.5\pm0.1$ K.

At last, at the third stage, we determine the behavior of extensive and intensive BCE at T_2 taken into account the peculiarities of experiments with DTA under pressure. As it was discussed above, increase in pressure strongly decreases the entropy jump δS_2 at the first order phase transition $Pc - P1$ (Fig. 2(b) and (d)), while the total entropy change ΔS_2 remains constant. Analyzing the dependencies $S(T, p)$ using both the DTA data under pressure and the effect of the lattice expansion, barocaloric parameters at T_2 are determined and presented in Fig. 5 in comparison with the data obtained in the second stage. One can see that in this case the magnitudes of $(\Delta S^{max}_{BCE})_{T2}$ and $(\Delta T^{max}_{AD})_{T2}$ are realized at almost the same low pressure which was determined in the second stage (Fig. 4(c) and (d)). The main difference was observed in the form of peaks $(\Delta S_{BCE})_{T2}(T)$ and $(\Delta T_{AD})_{T2}(T)$ which is due to peculiarities of the processes of measuring the heat capacity by methods of adiabatic calorimeter and DTA.

Returning to the results of the BCE study at T_1, one can confidently argue that it would be interesting and useful to investigate the influence of the thermal expansion of the crystal lattice on conventional BCE in ferroelectrics characterized by large β_{LAT} and undergoing order–disorder transformation with the positive baric coefficient.

4. Conclusion

This paper demonstrates BCE in NH_4HSO_4 undergoing two successive ferroelectric phase transitions characterized by significantly different entropy changes (ΔS_1=1.2 J/mol•K, $\Delta S_2 = 7.6$ J/mol•K) and large baric coefficients of different sign (dT_1/dp=+90 K/GPa and dT_2/dp = -123 K/GPa). Hydrostatic pressure strongly decreases the entropy jump at T_2 which reaches zero at a pressure of 0.17 GPa. Very low pressure is needed to realize the

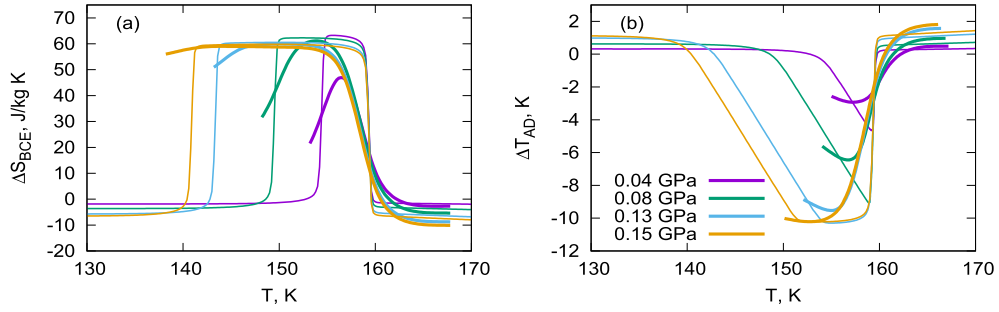

Fig. 5. (a) Barocaloric entropy and (b) adiabatic temperature changes at different hydrostatic pressure determined using DTA data on a jump of the entropy (thick lines) and data presented in Fig, 4(c) and (d) (thin lines).

maximum values of the extensive and intensive inverse BCE. Large thermal expansion of the crystal lattice leads to two very important points. Firstly, the conventional BCE can be greatly increased to values much higher than the magnitudes corresponding to the entropy of the phase transition. Secondly, in the case of the negative baric coefficient, a conversion from the inverse to conventional BCE can be realized by low pressure in the narrow temperature range.

References

[1] K.A. GschneidnerJr, V.K. Pecharsky, A.O. Tsokol, Recent developments in magnetocaloric materials, Rep. Prog. Phys. 68 (6) (2005) 1479–1539, https://doi.org/10.1088/0034-4885/68/6/r04.

[2] M. Valant, Electrocaloric materials for future solid-state refrigeration technologies, Prog. Mater. Sci. 57 (6) (2012) 980–1009, https://doi.org/10.1016/j.pmatsci.2012.02.001.

[3] X. Moya, S. Kar-Narayan, N.D. Mathur, Caloric materials near ferroic phase transitions, Nat. Mater. 13 (2014) 439–450, https://doi.org/10.1038/nmat3951.

[4] H. Khassaf, T. Patel, R.J. Hebert, S.P. Alpay, Flexocaloric response of epitaxial ferroelectric films, J. Appl. Phys. 123 (2) (2018), https://doi.org/10.1063/1.5009121, 024102.

[5] U. Tomc, J. Tušek, A. Kitanovski, A. Poredoš, A new magnetocaloric refrigeration principle with solid-state thermoelectric thermal diodes, Appl. Therm. Eng. 58 (1) (2013) 1–10, https://doi.org/10.1016/j.applthermaleng.2013.03.063.

[6] U. Plaznik, M. Vrabelj, Z. Kutnjak, B. Malič, A. Poredoš, A. Kitanovski, Electrocaloric cooling: the importance of electric-energy recovery and heat regeneration, Europhys. Lett. 111 (5) (2015) 57009, https://doi.org/10.1209/0295-5075/111/57009.

[7] A. Kitanovski, U. Plaznik, U. Tomc, A. Poredoš, Present and future caloric refrigeration and heat-pump technologies, Int. J. Refrig. 57 (2015) 288–298, https://doi.org/10.1016/j.ijrefrig.2015.06.008.

[8] N. Michaelis, F. Welsch, S.-M. Kirsch, M. Schmidt, S. Seelecke, A. Schütze, Experimental parameter identification for elastocaloric air cooling, Int. J. Refrig. 100 (2019) 167–174, https://doi.org/10.1016/j.ijrefrig.2019.01.006.

[9] M. Gorev, E. Bogdanov, I. Flerov, T-p phase diagrams and the barocaloric effect in materials with successive phase transitions, J. Phys. D Appl. Phys. 50 (38) (2017) 384002, https://doi.org/10.1088/1361-6463/aa8025.

[10] M. Gorev, E. Bogdanov, I. Flerov, Conventional and inverse barocaloric effects around triple points in ferroelastics $(NH_4)_3NbOF_6$ and $(NH_4)_3TiOF_5$, Scr. Mater. 139 (2017) 53–57, https://doi.org/10.1016/j.scriptamat.2017.06.022.

[11] E. Mikhaleva, I. Flerov, A. Kartashev, M. Gorev, A. Cherepakhin, K. Sablina, N. Mikhashenok, N. Volkov, A. Shabanov, Caloric effects and phase transitions in ferromagnetic-ferroelectric composites $xLa_{0.7}Pb_{0.3}MnO_3$-(1-x)$PbTiO_3$, J. Mater. Res. 28 (24) (2013) 3322–3331, https://doi.org/10.1557/jmr.2013.360.

[12] K. Alex Müller, F. Fauth, S. Fischer, M. Koch, A. Furrer, P. Lacorre, Cooling by adiabatic pressure application in $Pr_{1-x}La_xNiO_3$, Appl. Phys. Lett. 73 (8) (1998) 1056–1058, https://doi.org/10.1063/1.122083.

[13] T. Strässle, A. Furrer, Z. Hossain, C. Geibel, Magnetic cooling by the application of external pressure in rare-earth compounds, Phys. Rev. B 67 (2003), https://doi.org/10.1103/PhysRevB.67.054407, 054407.

[14] N.A. de Oliveira, Barocaloric effect and the pressure induced solid state refrigerator, J. Appl. Phys. 109 (5) (2011), https://doi.org/10.1063/1.3556740, 053515.

[15] P. Lloveras, E. Stern-Taulats, M. Barrio, J.-L. Tamarit, S. Crossley, W. Li, V. Pomjakushin, A. Planes, L. Manosa, N.D. Mathur, X. Moya, Giant barocaloric effects at low pressure in ferrielectric ammonium sulphate, Nat. Commun. 6 (2015), https://doi.org/10.1038/ncomms9801, 8801.

[16] H. Khassaf, T. Patel, S.P. Alpay, Combined intrinsic elastocaloric and electrocaloric properties of ferroelectrics, J. Appl. Phys. 121 (14) (2017), https://doi.org/10.1063/1.4980098, 144102.

[17] Y. Liu, J. Wei, P.-E. Janolin, I.C. Infante, X. Lou, B. Dkhil, Giant room-temperature barocaloric effect and pressure-mediated electrocaloric effect in $BaTiO_3$ single crystal, Appl. Phys. Lett. 104 (16) (2014), https://doi.org/10.1063/1.4873162, 162904.

[18] M.V. Gorev, I.N. Flerov, E.V. Bogdanov, V.N. Voronov, N.M. Laptash, Barocaloric effect near the structural phase transition in the Rb_2KTiOF_5 oxyfluoride, Phys. Solid State 52 (2) (2010) 377–383, https://doi.org/10.1134/S1063783410020253.

[19] E. Mikhaleva, I. Flerov, A. Kartashev, M. Gorev, E. Bogdanov, V. Bondarev, Thermal, dielectric and barocaloric properties of NH_4HSO_4 crystallized from an aqueous solution and the melt, Solid State Sci. 67 (2017) 1–7, https://doi.org/10.1016/j.solidstatesciences.2017.03.004.

[20] R. Pepinsky, K. Vedam, S. Hoshino, Y. Okaya, Ammonium hydrogen sulfate: a new ferroelectric with low coercive field, Phys. Rev. 111 (1958) 1508–1510, https://doi.org/10.1103/PhysRev.111.1508.

[21] D. Swain, V.S. Bhadram, P. Chowdhury, C. Narayana, Raman and x-ray investigations of ferroelectric phase transition in NH_4HSO_4, J. Phys. Chem. A 116 (2012) 223–230, https://doi.org/10.1021/jp2075868.

[22] R. Pirc, Z. Kutnjak, R. Blinc, Q.M. Zhang, Upper bounds on the electrocaloric effect in polar solids, Appl. Phys. Lett. 98 (2) (2011), https://doi.org/10.1063/1.3543628, 021909.